Location of Pupil Contour by Hough Transform of Connectivity Components

Ivan Matveev[1,3], Nikolay Chinaev[2] and Vladimir Novik [3]
[1]*Computing Centre of Russian Academy of Sciences, Vavilov str., 40, Moscow, 119333, Russia*
[2]*Moscow Institute of Physics and Technology, Institutsky per., 9, Dolgoprudny, 141700, Russia*
[3]*Iritech Inc., B.Tatarskaya str., 21, 115184, Russia*

Keywords: Iris Segmentation, Hough Transform.

Abstract: A method for determining the pupil boundary in the image of eye is proposed. The method is based on image binarization followed by a search of the pupil as one of the connectivity components. The pupil boundary is determined as a part of boundary of the connectivity component. Hough transform is used for separating pupil in the case of its merging in one connectivity component with other objects, as well as to verify the likelihood of solution.

1 INTRODUCTION

Iris region segmentation in eye images is an interesting and actual task for biometric identification and medical applications. An important sub-task is detection of pupil boundaries that is in fact search for rounded dark object. Circle detection is one of the most popular problems in image processing field. Numerous different methods have been developed, some of which are applicable in the particular case of pupil border detection. One can outline morphology methods (Bowyer et al., 2008), projections of brightness and its gradient (Matveev, 2010; Mohammed et al., 2010), optimal contour construction (Ritter and Cooper, 2003). Big share of methods (Matveev, 2012; Chen et al., 2012; Ma et al., 2002; Pan et al., 2011) relies on Hough transform (Hough, 1959) ideology.

The essence of this transform is the following: when searching for parametrically defined object (circle, straight line, ellipse, etc.) the space of parameters is considered, called *accumulator*. For instance, arbitrary circle is given by an equation $(x-x_0)^2+(y-y_0)^2=r^2$ with three parameters $(x_0,y_0,r)=\vec{p}$. Consequently three-dimensional accumulator is considered. A *counter function* $A(\vec{p})$ is defined in the accumulator, initially zero in all its points. The pixels which can be part of the searched figure are determined in the processed image, call them *candidates*. For example, when searching for circles pixels with high brightness gradient can be assumed as belonging to the circle border and marked as candidates, whereas pixels with low gradient belong to circle border less likely. A *voting* procedure is conducted: for each candidate a set of points in the accumulator is treated, corresponding to all possible parameters of the figures, which may include this candidate, the counter value at these points is incremented. Then maximum (or several local maxima) of the counter are determined, its position in the accumulator space defines the parameters of the searched figure. The advantage of Hough transform is its stability against partial occlusion of the figure, for example, it can be used to find the circumference by one of its arcs. The drawback is a relatively high computational cost arising from complex processing of candidates.

Morphology and brightness projection based object detection methods often apply brightness thresholding (or more elaborate techniques) as the first step to create binarized image, which is then processed. This is done under assumption that pixels of object region have uniform characteristics, which are distinct from those of background. Pixels with similar characteristics usually form several blobs in image, call them *connectivity components*. As a rule, pupil is a darkest object in eye image that prompts to apply binarization by brightness level and then detect roundish black connectivity component in black-and-white binarized image. Since binarization and extracting connectivity components are computationally simple procedures, the advantages of this method is the execution speed. It should be noted that the borders of objects appearing in binarization consist of a

Matveev I., Chinaev N. and Novik V..
Location of Pupil Contour by Hough Transform of Connectivity Components.
DOI: 10.5220/0005456100140021
In *Proceedings of the 5th International Workshop on Image Mining. Theory and Applications* (IMTA-5-2015), pages 14-21
ISBN: 978-989-758-094-9

relatively small number of pixels. However, quite often binarization generates several connectivity components, as the brightness of the eyebrows or eyelashes may be a little different from the brightness of the pupil or even be lower. Also eyelashes and eyelids may merge with the pupil to form one component of inadequate form. Therefore, the disadvantage of this class of methods is a significant share of errors associated with the distortion of the shape of object, arising from merging with stranger objects or removing parts of genuine object.

The presented work attempts to combine the advantages of the method of binarization, which retrieves a small number of pixels of interest in the image, and Hough transform, which extracts the shape of a given type from very noisy data. On the binarized image connectivity components are outlined, boundary of each is subjected to Hough transform to find the rounded contours. This combination of methods is not known to the authors from literature.

2 PROBLEM STATEMENT AND SOLUTION METHOD

Image of eye with the surrounding parts of the face (eyebrows, nose, cheeks part) is considered. Image is grayscale, i.e. contains only one luminosity channel. Typically it is registered in IR range. It is necessary to find a circle, which is the best approximation of the boundary between pupil and iris. The border can be partially occluded by eyelashes, eyelids, reflections. Pupil is dark but not necessarily darkest object in image, see Fig.1. Define source raster image

(a) (b)

Figure 1: Samples of eye images.

$I(x,y) = I(\vec{p})$, its size is $W \times H$ pixels. It is necessary to find coordinates and radius of circle, which approximates pupil.

The workflow of method is presented in the block diagram, see Fig.2. Now we describe it briefly and in the following subsections more details are given.

Several thresholds of binarization B_k are calculated from image brightness histogram (block 1). Connectivity components corresponding to the dark areas are outlined by binarization (block 2). For each component its boundary and inertia moments are determined (block 3). Moments of the component are used to calculate the likelihood that pupil belongs to a this component, then components are sorted so as to process ones with highest likelihood first (block 4). The boundary of each component is a cyclic sequence of edges, see more details in section 2.7. It should be noted that the number of border edges is substantially smaller than their total number in the image or the number of pixels with high brightness gradient, which could be considered as parts of boundary. The pupil not always has border with lighter iris only, but is often covered with eyelids and / or eyelashes that causes distortions of two kinds: the boundary of the pupil is visible partially; connectivity component of pupil merges with eyelids or eyelashes (see. Fig. 1 (b)). In this case only a small part of detected boundary belongs to pupil, however it is necessary to determine visible part of the boundary. Hough transform is performed (block 5), which includes construction of beams in the accumulator starting from each pixel of boundary perpendicular to it. As a result, if the boundary contains circular arc, significant local maxima arise in the accumulator at the center of hypothetical circle containing these arc. Global maximum of accumulator corresponds to the most likely position of the circle. To determine the radius of the circle histogram of distances from the found center to the boundary pixels is built (block 6). Maximum of the histogram gives the radius. Following subsections describe steps of the method in more detail.

2.1 Estimating Binarization Thresholds

As the pupil is dark image area, it can be outlined as a connectivity component when the binarization threshold value exceeds pupil brightness and is below iris brightness. Boundary of this connectivity component is a pupil border. As levels of brightness of pupil and iris are unknown a-priory, and hence the threshold dividing them is also unknown, several passes (denoted their count as K) of algorithm with different thresholds are performed. The values of applied thresholds are determined so that the number of pixels with brightness below the threshold is a certain fraction of the total pixel number. For this purpose brightness histogram is used:

$$h(b) = |\{\vec{p} : I(\vec{p}) \leqslant b\}| \ . \qquad (1)$$

Pupil is a dark object, so histogram part corresponding to the low brightness is analysed. Shares of pixels α_k, determining the binarization thresholds, are set

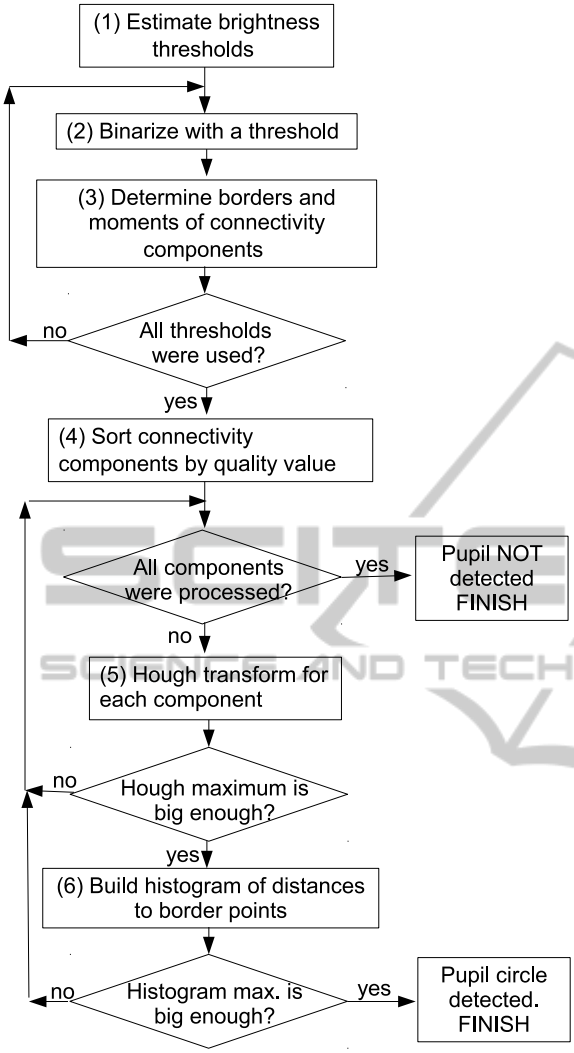

Figure 2: Block diagram of method functioning.

uniformly in range from 0 to $1/4$ of total pixel count:

$$\alpha_k = \frac{1}{4}\frac{k}{K}, k = 1,\ldots,K \ . \tag{2}$$

Binarization thresholds B_k are calculated by histogram (1) and shares (2):

$$B_k : h(B_k) = \alpha_k WH \ . \tag{3}$$

2.2 Binarization

Binarization with threshold B is performed to zero brightnesses over the threshold and outline the pixel with lower intensities so as to generate objects from dark regions:

$$I_B(\vec{p}) = \begin{cases} 1, & I(\vec{p}) \leqslant B \ , \\ 0, & otherwise \ . \end{cases} \tag{4}$$

Samples of binarized images I_B are given in Fig.3

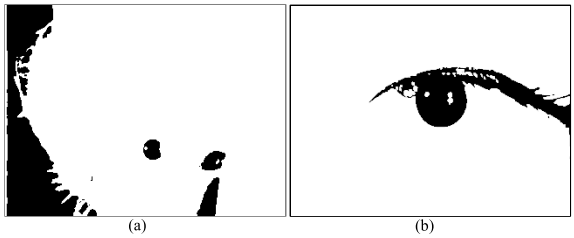

Figure 3: Samples of binarized images. (a) — image obtained from Fig.1a with share of pixels $\alpha_k = 0.14$; (b) — image, obtained from Fig.1b with share of pixels $\alpha_k = 0.08$.

2.3 Determining Borders and Moments of Connectivity Components

In the binarized image dark (the brightness is less than the threshold) and light areas form several connectivity components. Here 8-connectivity is used i.e. dark pixels $\vec{q}$ are considered connected with pixel $\vec{p}$, $I_B(\vec{p}) = 1$, if $\vec{q}$: $I_B(\vec{q}) = 1$, $|p_x - q_x| \leqslant 1$, $|p_y - q_y| \leqslant 1$. For each connectivity component C ordered list of border edges $L(C) = \left\{\vec{l}_i\right\}$ and moments of zero order $M(C)$, first order $M_x(C)$, $M_y(C)$ and second order are calculated:

$$\begin{gathered} M(C) = |C| \equiv |\{\vec{p} : \vec{p} \in C\}| \ , \\ M_x(C) = \sum_{\vec{p}\in C} p_x \ , \ M_y(C) = \sum_{\vec{p}\in C} p_y \ , \\ M_{xx}(C) = \sum_{\vec{p}\in C} p_x^2 \ , \ M_{yy}(C) = \sum_{\vec{p}\in C} p_y^2 \ , \\ M_{xy}(C) = \sum_{\vec{p}\in C} p_x p_y \ . \end{gathered} \tag{5}$$

Moments (5) are determined by enumerating all pixels of the component by the floodfill method (Glassner, 1990). List of border edges is determined by a special algorithm described in the section 2.7.

2.4 Rejection and Sorting of Connectivity Components

Components detected by binarization are subjected to Hough transform. However, some of them can be discarded before the processing merely by the statistical characteristics as obviously not containing the pupil, and the remaining can be sorted, so that the first processed components contain pupil with the highest probability. To remove components, obviously not containing the pupil parameters of *equivalent ellipse* are considered. They are calculated as:

$$
\begin{aligned}
&a = \left(p^2\overline{M}_{xx} + 2pq\overline{M}_{xy} + q^2\overline{M}_{yy}\right)^{1/2},\\
&b = \left(q^2\overline{M}_{xx} - 2pq\overline{M}_{xy} + p^2\overline{M}_{yy}\right)^{1/2},\\
&p = \cos\varphi\,,\quad q = \sin\varphi\,,\\
&\varphi = \tfrac{1}{2}\arctan\tfrac{2\overline{M}_{xy}}{\overline{M}_{xx}-\overline{M}_{yy}},\\
&\overline{M}_{xx} = \tfrac{M_{xx}}{M} - \left(\tfrac{M_x}{M}\right)^2,\\
&\overline{M}_{xy} = \tfrac{M_{xy}}{M} - \tfrac{M_x M_y}{M^2},\\
&\overline{M}_{yy} = \tfrac{M_{yy}}{M} - \left(\tfrac{M_y}{M}\right)^2,
\end{aligned}
\tag{6}
$$

where a, b, φ are big and small half-axes and direction of big half-axis respectively. Connectivity component containing pupil should have a sufficiently large area, and the ratio of the major and minor semi-axes must lie within a certain range. Furthermore, if eyelashes / eyelids have same or smaller brightness than the pupil, induced distortion of the connectivity component extends it horizontally but not vertically. Accordingly, the objects with equivalent ellipse having large eccentricity and major axis located closer to the vertical should be discarded. These conditions are written as:

$$
\begin{aligned}
&ab > \rho_{min}^2\ ,\\
&\frac{a}{b} < T_1\ ,\\
&\neg\left(\left(\frac{a}{b} > T_2\right)\cap\left(\varphi\in\left[\frac{\pi}{4};\frac{3\pi}{4}\right]\right)\right)\ ,
\end{aligned}
\tag{7}
$$

where ρ_{min} is minimal possible radius of pupil in pixels. Optimal values of thresholds $T_1 = 5$, $T_2 = 2.5$ are determined experimentally.

To sort residual components the following quality criteria is calculated:

$$
\Theta(C) = \frac{M(C) - l(C)}{l^2(C)}\ , \tag{8}
$$

where $l(C) = |L(C)|$ is a length of connectivity component border. This feature increases as the shape of the region approximates to the circular, and also increases with the size of the area. Thus, connectivity components are sorted by descending characteristic (8), which favours rounded components of significant size.

2.5 Hough Transform

Voting procedure is performed as follows: inner normals to each pixel $\vec{l}_i \in L$ are constructed, a segment of normal enclosed in range $[\rho_{min};\rho_{max}]$ is selected, counter function in appropriate accumulator points is increased.

$$
\begin{aligned}
&A(\vec{p}) := A(\vec{p}) + v(\vec{p},\vec{l}_i),\\
&v(\vec{p},\vec{l}_i) = \begin{cases} 1, & if\ \vec{p} = r\vec{\eta} + \vec{l}_i,\\ & r\in[\rho_{min};\rho_{max}];\\ 0, & otherwise\,. \end{cases}
\end{aligned}
\tag{9}
$$

Constructing normal vector $\vec{\eta}$ is done as follows: closest neighbours of pixel $\vec{l}_i$ in list L are selected, define them as $\vec{l}_j$, where negative index corresponds to moving backward in the list and positive is forward. Tangent direction $\vec{\tau}$ is estimated from the neighbour pixel coordinates:

$$
\vec{\tau} = \sum_{j=-n}^{-1}\frac{\vec{l}_i - \vec{l}_j}{\left|\vec{l}_i - \vec{l}_j\right|} + \sum_{j=1}^{n}\frac{\vec{l}_j - \vec{l}_i}{\left|\vec{l}_j - \vec{l}_i\right|}\ , \tag{10}
$$

where n is a size of pixel neighbourhood and is equal to $\rho_{min}/2$. From two possible normal directions $\vec{\eta}_1 = (\eta_x,\eta_y) = (-\tau_y,\tau_x)$ and $\vec{\eta}_2 = (\tau_y,-\tau_x)$ inner normal is selected according to direction of border enumeration. Segment for voting is constructed in rastered accumulator by Bresenham algorithm (Bresenham, 1996). After the voting the accumulator is smoothed by the low-pass filter and center of the hypothetical circle is determined as the global maximum in smoothed accumulator:

$$
\vec{c} = arg\max_{\vec{p}}\left(A(\vec{p}) * G\right)\ , \tag{11}
$$

where G is a low-pass filter. Fig. 4 (a) depicts a results of Hough transform for biggest connectivity component of image Fig. 3 (b), which contains pupil. This is the only component for processing, others were rejected at the previous stage.

2.6 Building Histogram of Distances to Border Edges

A histogram $h(r)$ of distances from center $\vec{c}$ and all edges of the border $L = \left\{\vec{l}_i\right\}$ is constructed:

$$
h(r) = \left|\left\{\vec{l}_i : \vec{l}_i \in L, r - 0.5 \leqslant \|\vec{c} - \vec{l}_i\| < r + 0.5\right\}\right|. \tag{12}
$$

Histogram has a specific properties in case when pupil belongs to the component and its center is correctly detected. For instance in Fig. 4 (b), a histogram for component Fig. 3 (b) is given. One can see a peak corresponding to the radius of pupil in image: $r_P = arg\max_r h(r)$. The final conclusion about pupil presence is based on analysis of $h(r)$. Mass of the histogram is calculated in window of width w centered at r_P, which is position of histogram maximum. The resulting value is an estimate of the length of the visible contour of the pupil, and is compared with r_P. Is is considered that pupil is detected if

$$
\sum_{r=r_P-w}^{r_P+w} h(r) > \pi r_P\ , \tag{13}
$$

i.e. sufficient condition for pupil detection is visibility of half of its border. the width w of the summing

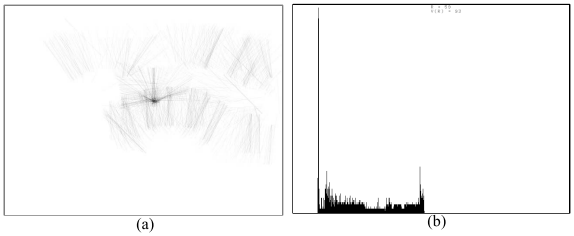

Figure 4: Processing of connectivity components. (a) — result of voting by component of image 3 (b) with maximum Θ value and satisfying conditions (7); (b) — histogram of distances (12) from hypothetical center of circle to border edges.

window depends on precision of center detection, it is set here to $w = 2$ according to numerical tests.

So, the method includes the following steps:

S t e p 1. Building brightness histogram (1). Calculating binarization thresholds B_k according to (3).

For each k steps $2-3$ are carried out.

S t e p 2. Image binarization (4) with threshold B_k.

S t e p 3. Determining moments (5) and borders of each connectivity components, rejecting those unfit to (7).

S t e p 4. Sorting of residual components according quality criterion (8).

Following steps $5-6$ are executed subsequently for elements of sorted list, until an element satisfying conditions is met (as a rule it is the first one in the list) of the list is exhausted.

S t e p 5. Hough transform (9) for borders, maximum (11) is detected.

S t e p 6. If maximum is sufficiently large, histogram (12) is built. If peak (13) exists in the histogram, it means that roundish segment of border exists with center close to detected accumulator maxima and radius equal to coordinate of the peak. If no component satisfies these conditions, it is declared that no pupil is present in the image.

2.7 Algorithm of Border Edges Enumeration

Here the algorithm of building list L of border edges of connectivity component C is presented. It works in binarized image and treats the object and its border under 8-connectivity assumption. The algorithm is executed by a finite state automaton, which diagram is given in Fig. 5. Binarized image (4) is scanned as a raster until non-zero pixel $\vec{p}$: $I_B(\vec{p}) = 1$ is detected. It means new connectivity component is encountered. The enumeration of border edges starts followed by enumeration and zeroing of all object pixels by a floodfill procedure (Glassner, 1990). Dur-

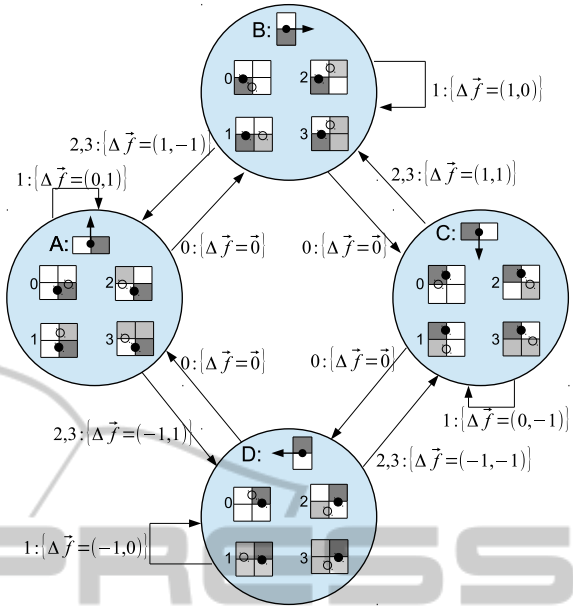

Figure 5: Automaton diagram for border pixel enumeration.

ing the floodfill procedure the object is cleaned from the image. Enumeration of border edges is done sequentially, starting from first detected one. At each step of automaton work there is one currently processed pixel $\vec{f}$, call it *focus pixel*. When first pixel of object is encountered during raster scanning it has configuration "A".Finite automaton has four states corresponding to four border orientations and directions of movements along the border. Border enumeration is done clockwise. Four states are: "A" — left border, movement upwards; "B" — upper border, movement rightward; "C" — right border, movement downwards; "D" — low border, movement leftwards. In each state there are four possible configurations of neighbourhood, denoted by numbers from 0 to 3 and three directions of subsequent movement: turn to the right (executed in configuration 0), continue moving without changing direction (configuration 1) and turn to the left (configurations 2 and 3). Automaton state is changed according to new direction in case of turns or remains unchanged in case of direct movement. Focus pixel is changed for configurations 1, 2 and 3 or remains the same for configuration 0. Each new edge is added to the list L. If new edge coincide to the first one in the list, it means that the enumeration of border is completed and the automaton is stopped.

The sample of object is given in Figure 6. The first detected pixel of object is border pixel number "1", which is set as initial focus pixel and the first enumerated edge is "a". The automaton is set to configuration "A". Neighbourhood configuration is 0, thus the automaton changes state to "B" (right turn) and pro-

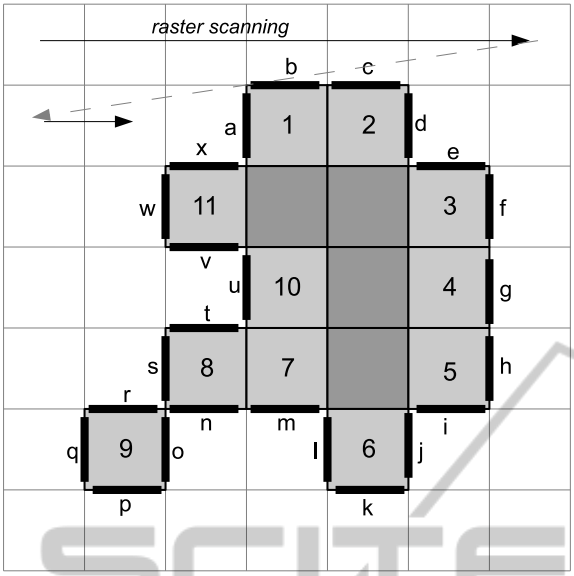

Figure 6: Sample of object, its border pixels and edges.

ceeds to edge "b", focus pixel remains unchanged at this step. Proceeding further will finally enumerate edges from "a" to "x" as shown in alphabetical order and pixels in order $1,2,3,4,5,6,7,8,9,8,10,11$.

2.8 Estimation of Algorithmic Complexity

Image size if $W \times H$, W H, and the width of image W can be considered as image linear size, thus number of image pixels is proportional to W^2.

Estimation of binarization thresholds includes building and processing brightness histogram with complexity $\max\{W^2, L\}$, where L is a number of brightness levels in image. Grayscale 8-bit images are used hence $L = 256 \ll W^2$. Binarization and connectivity component selection for one binarization threshold have complexity W^2. Number of connectivity components is limited by W^2/ρ_{min}^2, where ρ_{min} is a minimum expected pupil radius. Length of the border can be evaluated as W. Total complexity of K passes of binarization is KW^2, as a result KW^2/ρ_{min}^2 connectivity components are extracted. Hough voting for one pixel has complexity of W, and for whole border it is W^2. Maxima search in accumulator requires W^2 operations. Thus, considering the above total complexity of the method comprises kW^4/ρ_{min}^2.

With the increase of image resolution and its linear size W expected pupil size also grows linearly, so one can state that ρ_{min} W and the complexity of the algorithm is in fact kW^2. It grows linearly with respect to image pixel number. Direct application of Hough transform to locate circle yields complexity of W^3. The reduction of complexity in the proposed approach is produced by using preselected border pixels, which number is proportional to W, instead of treating all image pixels (or some share of them selected by thresholding), which number is proportional to W^2.

3 EXPERIMENTS

Four public domain iris image databases were used for tests, defined as:

- BATH (Monro et al., 2005);
- CASIA (Chinese Academy of Sciences Institute of Automation, 2005);
- MMU (Multimedia University, 2006);
- NDIRIS (Phillips et al., 2010).

These images were marked by a human expert: in each a circle approximating pupil border was set. Define center of such circle as (x_0, y_0) and its radius r_0. Algorithm detected center (x, y) and radius r of pupil circle in each image and these data were matched against expert ones, the deviation of center was calculated as $Q_C = |x_0 - x| + |y_0 - y|$ and the deviation of radius as $Q_R = |r - r_0|$. Table 1 represents comparison of the method with its analogues. Three methods were used, which results are known from literature. They are referenced in the table as

- column 1 (Masek, 2003);
- column 2 (Ma et al., 2004);
- column 3 (Daugman, 2007);
- column 4 - method presented here.

The following characteristics are given: average deviation of pupil center $\overline{Q}_C$ (average value of Q_C for all test set), average radius deviation $\overline{Q}_R$, both expressed in pixels, and mean calculation time $\overline{T}$, expressed in milliseconds.

Table 1: Comparison with other methods.

DB	Values	Methods			
		1	2	3	4
BATH	$\overline{Q}_C$	5.32	4.29	3.27	4.61
	$\overline{Q}_R$	6.72	4.65	3.19	1.59
	$\overline{T}$	108.26	376.83	26.55	97.28
CASIA	$\overline{Q}_C$	3.67	4.79	1.19	2.82
	$\overline{Q}_R$	5.15	5.39	3.02	3.26
	$\overline{T}$	97.52	363.64	29.17	93.95
MMU	$\overline{Q}_C$	4.98	3.92	1.14	3.11
	$\overline{Q}_R$	5.78	4.67	3.76	0.99
	$\overline{T}$	99.78	317.18	25.47	25.22
NDIRIS	$\overline{Q}_C$	5.59	5.92	1.79	3.94
	$\overline{Q}_R$	7.23	7.38	3.11	1.89
	$\overline{T}$	112.25	378.87	27.61	98.30

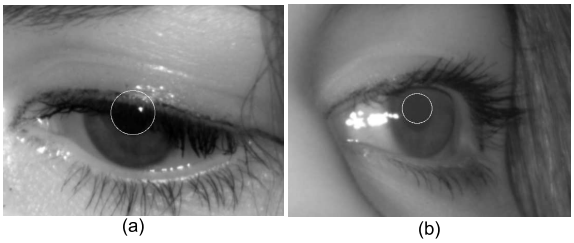

(a) (b)

Figure 7: Sample correct detection in case of occlusion and virtually correct detection in case of side gaze.

Figure 7 gives examples of correct detection of pupil. Most typical error is mistaking iris border for pupil border, which can result in case of low contrast of iris-pupil border (see Figure 8a), and occlusion of the pupil (see Figure 8b). Comparing Fig.8b with Fig.7a one can note that the share of pupil border visible in Fig.8b is bigger thn that of in Fig.7a, but detection is wrong due to mistaking iris border, which is visible in bigger part. The third biggest problem for

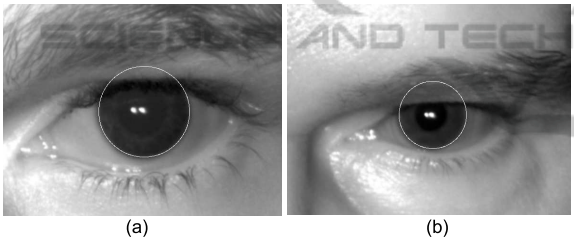

(a) (b)

Figure 8: Sample incorrect detection in case of low contrast of pupil-iris border and occlusion.

the algorithm is off-side gazing. When gazing causes pupil to deform strongly, Hough voting for circle fails to produce maxima in the contour center. Again, the most frequent result is mistaking iris for pupil, see Figure 9a. An interesting case is that of red eye effect, see Figure 9b.

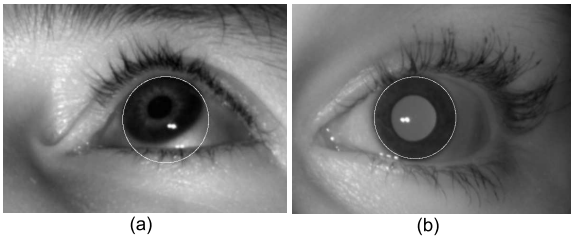

(a) (b)

Figure 9: Sample incorrect detection in case of low contrast of pupil-iris border and occlusion.

4 CONCLUSIONS

Method of pupil contour detection in eye image is proposed. Contour is built from pixels of boundary of connectivity component obtained from a dark region in source image. To select correct (closest to the circle) component (or part thereof) Hough transform of boundary pixels is used, yielding the center of circular part of border. Radius of the circle is defined as the maximum of the histogram of distances of boundary pixels to a dedicated center. Then pupil contour pixels may be selected from the entire set of pixels of the boundary as being close to that radius distance to the center. Tests of the algorithm were performed on sets of images of public domain databases. Using the Hough transform one can correctly locate the true center, radius and contour of the pupil, even in the presence of high interference, provided only partially visible contour of the pupil. The disadvantage of this method is potentially great execution time, which may occur when iterating through many connectivity components and several binarization thresholds. This drawback is partially mitigated by using quality measure of connectivity components.

ACKNOWLEDGEMENTS

The work was funded by RFBR grant No.14-01-00348.

REFERENCES

Bowyer, K., Hollingsworth, K., and Flynn, P. (2008). Image understanding for iris biometrics: a survey. *Computer Vision and Image Understanding*, 110(2):281 307.

Bresenham, J. (1996). Pixel-processing fundamentals. *IEEE Comput Graphics Appl*, 16(1):74–82.

Chen, D., Bai, J., and Qu, Z. (2012). Research on pupil center location based on improved hough transform and edge gradient algorithm. *Proc. National Conf. Information Technology and Computer Science*, page 47 51.

Chinese Academy of Sciences Institute of Automation (2005). Iris image database, version 3.

Daugman, J. (2007). New methods in iris recognition. *IEEE Trans. Systems, Man and Cybernatics-Part B: Cybernatics*, 37:1167 1175.

Glassner, A. S. (1990). *Graphics Gems*. Academic Press, Inc., Orlando, FL, USA.

Hough, P. (1959). Machine analysis of bubble chamber pictures. *Conf.Proc.*, C590914:554–558.

Ma, L., Tan, T., Wang, Y., and Zhang, D. (2004). Local intensity variation analysis for iris recognition. *Pattern Recognition*, 37(6):1287–1298.

Ma, L., Wang, Y., and Tan, T. (2002). Iris recognition using circular symmetric filters. *Proc. 16th Int. Conf. Pattern Recognition*, 1(2):414 –417.

Masek, L. (2003). Recognition of human iris patterns for biometric identification. *http:// www.csse.uwa.edu.au/ pk/ studentprojects/ libor*.

Matveev, I. A. (2010). Detection of iris in image by interrelated maxima of brightness gradient projections. *Applied and Computational Mathematics*, 9(2):252 – 257.

Matveev, I. A. (2012). Iris center location using hough transform with two-dimensional parameter space. *Journal of Computer and Systems Sciences International*, 51(6):785 – 791.

Mohammed, G., Hong, B., and Jarjes, A. (2010). Accurate pupil features extraction based on new projection function. *Computing and Informatics*, 29:663 – 680.

Monro, D. M., Rakshit, S., and Zhang, D. (2005). Universtiy of bath, u.k. iris image database.

Multimedia University (2006). Mmu iris image database.

Pan, L., Chu, W., Saragih, J., and de la Torre, F. (2011). Fast and robust circular object detection with probabilistic pairwise voting. *Signal Processing Letters*, 18(11):639–642.

Phillips, P., Scruggs, W., and et al., O. A. (2010). Frvt2006 and ice2006 large-scale experimental results. *IEEE PAMI*, 5(32):831–846.

Ritter, N. J. and Cooper, J. R. (2003). Locating the iris: A first step to registration and identification. *Proc. 9th IASTED Int. Conf. Signal and Image Processing*, pages 507–512.